Available online at www.sciencedirect.com
ScienceDirect
Procedia Engineering 2 (2010) 2347–2356
Procedia Engineering
www.elsevier.com/locate/procedia

Fatigue 2010

Assessment of multiaxial fatigue life prediction methodologies for Inconel 718

M. Filippini[a,]*, S. Foletti[a], G. Pasquero[b]

[a]*Politecnico di Milano, Dipartimento di Meccanica, Via La Masa 1, 20156 Milano, Italy*
[b]*Avio S.p.A., Viale I Maggio 99, 10040 Rivalta di Torino, Italy*

Received 28 February 2010; revised 12 March 2010; accepted 15 March 2010

Abstract

Fatigue life prediction methodologies for the assessment of the structural integrity of safety critical components in modern turbine engines require a close integration of advanced multiaxial fatigue life prediction procedures and of specific multiaxial tests, representative of the service conditions of turbine engine components and materials. The objective of the research work presented in this paper is to extend currently employed methodologies for the assessment of fatigue strength of turbine engines disks by integrating suitable multiaxial fatigue criteria and test results of multiaxial fatigue experiments conducted on Inconel 718 material at temperatures similar to those experienced by the disc materials during service. Smooth tubular specimens of Inconel 718 have been employed for conducting tension/torsion strain controlled high temperature fatigue tests. Specimens have been cut out from forged parts utilised for the production of engine discs, thus preserving the typical properties of disc materials (microstructure, basic mechanical properties, etc.). Different models/criteria have been evaluated by comparing fatigue life predictions and multiaxial fatigue experiments. It's well known that agreement of life predictions with experimental life is strongly affected not only by the choice of the multiaxial fatigue criteria but also by the way the reference fatigue data are integrated in the criteria. Therefore, specific multiaxial fatigue tests have been carried out, in order to validate and to improve the assessment capabilities of the lifing procedures. Moreover, multiaxial fatigue tests permit advances in the basic understanding of materials behaviour that might be utilised in the processes of declaring component service lives.

Keywords: multiaxial fatigue; fatigue testing; high temperature testing; nickel alloys.

1. Introduction

Fatigue life prediction methodologies for the assessment of the structural integrity of safety critical components in modern turbine engines require a close integration of advanced multiaxial fatigue life prediction procedures and of specific multiaxial tests, representative of the service conditions of disc materials. In particular, multiaxial fatigue tests are required for checking their predictive capability in more complex stress state conditions, like those experienced by turbine engine components [1]-[4]. A research programme aimed at developing novel design methodologies for turbine engines disks has been carried out in cooperation between Politecnico di Milano

* Corresponding author. Tel.: +39-02-2399-8220; fax: +39-02-2399-8202.
E-mail address: mauro.filippini@polimi.it.

1877-7058
doi:10.1016/j.proeng.2010.03.251

(Technical University of Milano) and Avio S.p.A (Turin, Italy). The main objective of the programme is to extend currently employed methodologies for the assessment of fatigue strength of turbine engines disks by integrating suitable multiaxial fatigue criteria and test results of multiaxial fatigue experiments conducted at temperatures similar to those experienced by the disk materials during service.

In the effort of building a design tool, different models/criteria need to be evaluated by comparing fatigue life predictions and multiaxial fatigue experiments. It's well known that agreement of life predictions with experimental life is strongly affected not only by the choice of the multiaxial fatigue criteria but also by the way the reference fatigue data are integrated in the criteria [3], [4]. Therefore, it is of paramount importance conducting specific multiaxial fatigue tests, in order to validate and improve the assessment capabilities of the lifing procedures. Moreover, multiaxial fatigue tests permit advances in the basic understanding of materials behaviour that might be utilised in the processes of declaring component service lives. As a consequence, the research programme has been split into two parallel and interrelated activities: a modelling activity aimed at the choice and development of the most suitable criterion/method capable to address fatigue issues typical of disk materials, and an experimental campaign of multiaxial fatigue tests, for generating data for the improvement of predictive capability of fatigue criteria.

Smooth tubular specimens of Inconel 718 have been employed for conducting tension/torsion strain controlled high temperature fatigue test. The main advantage of tubular specimen over competing test technologies is due to the fact that they are more versatile, they easily permit to investigate material behaviour under non-proportional loading, they can be induction heated and they are relatively cheap to obtain. Moreover, stresses can be computed directly from the applied loads. Specimens have been cut out from forged parts utilised for the production of engine discs, thus preserving the typical properties of disc materials (microstructure, basic mechanical properties, etc.). In the present paper, the most relevant features of the research programme are outlined and the main results of the experimental campaign are presented. However, due to confidentiality issues, some experimental results are presented in normalised form.

Nomenclature

$\Delta\sigma_{ij}$	stress ranges
N_f	number of cycles to failure
$\sigma_{W,MM}$	equivalent stress in the Manson-McKnight model
m	Walker model exponent
$\bar{\theta}$, $\bar{\varphi}$	Euler angles identifying the critical plane
σ_{SWT}	equivalent stress in the Smith-Watson-Topper model
τ_{FS}	equivalent shear stress in the Fatemi-Socie model
σ_Y	tensile yield strength
$\sigma_{\max}$	maximum (over time) normal stress

2. Experiments

2.1. Material and specimen design

The material employed for conducting the fatigue tests have been extracted from a forged disk of Inconel 718. The forged parts have been selected from a set usually employed for the production of turbine engine disks, undergoing the vacuum melting, forging and heat treatment process of the engine disks, thus preserving the same

mechanical properties of the turbine engine disk alloys. Nominal chemical composition is reported in Table 1, while in Table 2 the room temperature monotonic properties are given.

Table 1. Average chemical composition (weight, %) of Inconel 718 alloy.

C	Cr	Mo	Ni	Ti	Al	Nb	Fe
0.03	19.00	3.10	53.00	0.95	0.55	5.30	19.00

Table 2. Room temperature monotonic properties of Inconel 718 alloy.

E [MPa]	$R_{p,0.2}$ [MPa]	R_m [MPa]	A %
205000	1150	1400	15

Specimens have been designed by taking into account the available testing technology and equipment and the possibility to extract a reasonable number of specimens out of an actual component (in un-machined condition). Tubular specimen geometry is shown in Fig. 1. The advantage of tubular specimen over competing technologies (e.g. cruciform specimens) is that they offer a uniform stresses gage length. Stresses can be calculated directly from the applied loads. A discussion of different multiaxial testing techniques can be found in [5]. Moreover, uniform temperature in the gage length in tubular specimens is easily achieved by induction heating, since relatively simple shape induction coils can be employed. The dimensions have been chosen by adapting the dimension ratios suggested by the ASTM E-2207 standard [6] to the need of optimising the extraction of specimens from the un-machined engine disks, to the available grips dimensions and to the load capacity of the testing equipment.

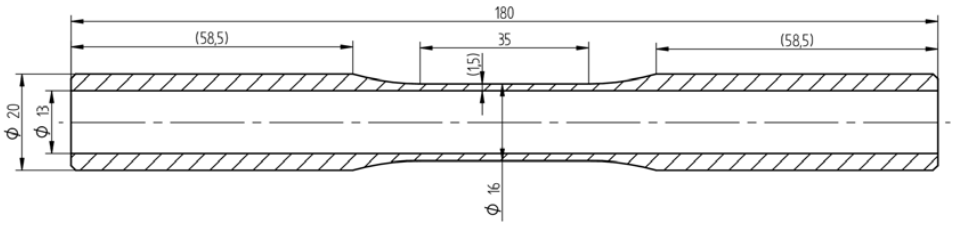

Fig. 1. Tubular specimen geometry and dimensions (in mm).

2.2. Fatigue test set-up and equipment

Strain controlled multiaxial fatigue tests have been performed at a temperature of 540 °C which represents the typical actual service condition of turbine engine disks (isothermal tests). In the tests, temperature is achieved by means of an induction heating furnace which is controlled by a thermocouple that needs to be welded onto the specimen surface. However, since spot welding of a thermocouple gives rise to a local stress concentration, the welded thermocouple could become the location of early fatigue failure during the tests. In order to avoid this, the controlling thermocouple shall not be welded in the gauge length of the specimen (ø= 16 mm), but in the gripping zone (ø= 20 mm), in correspondence of the end of the transition fillet. Consequently, a precise evaluation of temperature distribution in the specimen is needed for the correct control of the test temperature in the gauge length. Thermocouples (K type, 0.5 mm diam.) have been carefully welded on the surface of a dummy specimen, see Fig. 2.

Control thermocouple T_c is positioned at a distance of 2 mm from the fillet end, in the grip zone. Three thermocouples are symmetrically welded in the gauge length and a fourth one (T_4) is welded on the fillet region, opposite of the T_c. Spacing of the coil has been optimized so that a rather uniform temperature distribution in the gauge length could be achieved. However, even if quite limited, temperature differences in the gauge length are

observed ($T_{1\text{-}2\text{-}3}$), with a maximum difference ($\Delta T_{2\text{-}1}$) less than 2% of the maximum temperature in the mid section (T_2=540 °C), see Fig. 3.

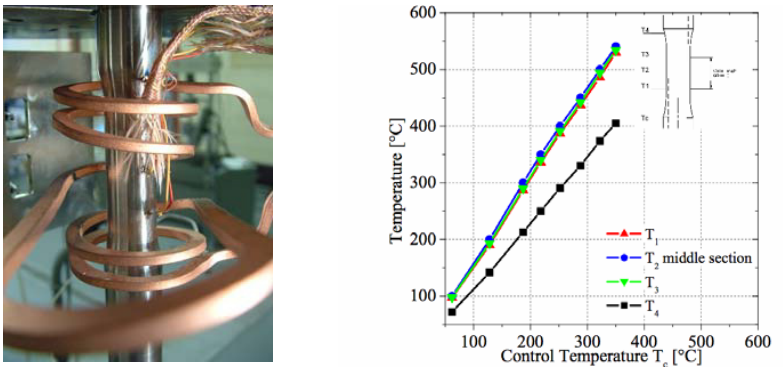

Fig. 2.(a) Closed view of the tubular specimen used for temperature setup; (b) measured temperature distribution on the specimen.

Uniaxial and multiaxial fatigue tests have been carried out by employing the fatigue testing equipment pictured in Figure 3. Fatigue tests have been carried out in strain control by employing as a control device a high temperature axial/torsional extensometer with a gauge length of 25 mm, see Fig. 3. By using the tools of the hardware and software electronics of the test equipment, a control software has been designed so that both control of the temperature and of the mechanical parameters (i.e. axial and shear stress-strain behaviour during the fatigue tests) could be managed through an integrated interface. A dummy specimen has been utilised for proper PID tuning of the test equipment for conducting strain controlled fatigue tests [7]. All fatigue tests have been carried out with a triangular wave shape at a frequency of 0.5 s^{-1}, except in the case of out-of-phase axial/torsional fatigue tests where a sinusoidal wave shape at 0.5 Hz has been applied.

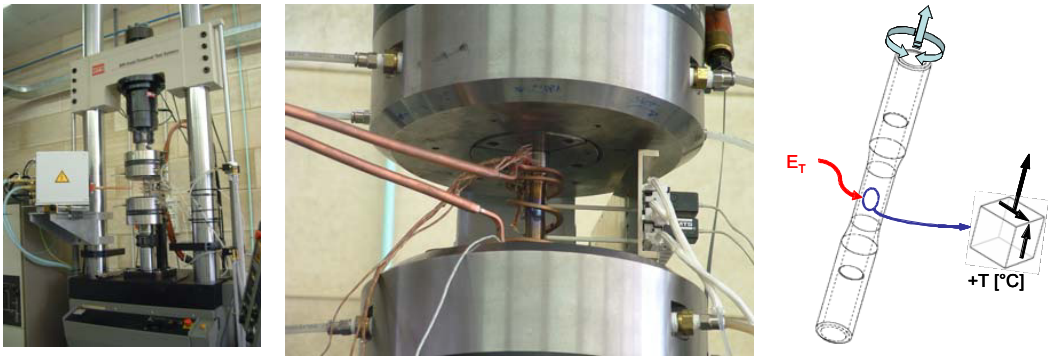

Fig. 3. Multiaxial (axial/torsional) fatigue testing equipment and applied strain.

2.3. Fatigue testing plan

Fatigue tests have been carried out with different load paths and strain ratios, according to the scheme shown in Fig. 4. The axial fatigue test have been conducted with applied strain ratio R_ε=-1, 0 and 0.5: the set of results with R_ε=-1 are needed to evaluate the parameters of the basic fatigue properties, i.e. the Manson-Coffin parameters and the stress-strain curve parameters, while fatigue tests results with R_ε=0 e R_ε=0.5 may be employed for identifying the specific parameters of different multiaxial fatigue life criteria and, in particular, to take into account of the effect

of mean stress (strain) on the fatigue life, [3], [4]. On the contrary, several multiaxial fatigue criteria, especially those based on the critical plane approach, need to identify the relevant fatigue properties on the basis of torsional fatigue data [4], [5]. Thus, shear strain controlled torsion fatigue tests have been conducted with two different strain ratios, R_γ=-1 e R_γ=0, in order to emphasize the effect, if present, of the mean shear stress on the fatigue life.

Moreover, strain controlled multiaxial fatigue tests have been carried out by imposing the load paths shown in Figure 5 (bottom row). Axial/torsional fatigue tests have been conducted with three different combinations of strain ratio: (i) R_ε=0, R_γ=-1; (ii) R_ε=0, R_γ=0; (iii) R_ε=0.5, R_γ=0. Only in the second case (ii), with both axial and shear strain R=0, the stress state is proportional with fixed principal directions, while both case (i) and (iii) can be classified as those of affine load paths. Finally, some axial/torsional strain controlled fatigue tests with non-proportional 90 degrees out-of-phase load paths have been performed, with two different combinations of strain ratio, (iv) R_ε=0, R_γ=-1; (v) R_ε=0, R_γ=0, so that a comparison with in-phase fatigue tests results (i, ii) could be made.

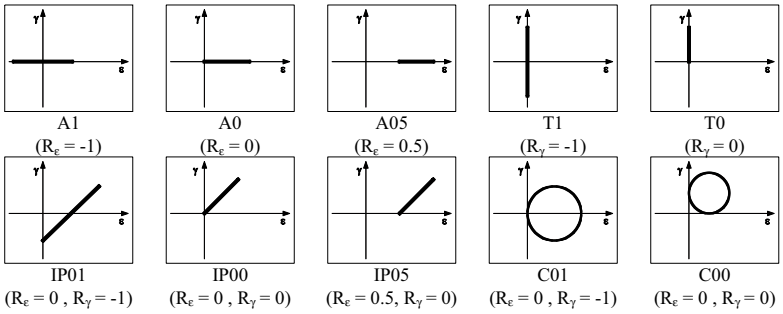

Fig. 4. Testing plan and loading paths applied during multiaxial fatigue tests.

In the case of axial/torsion strain controlled fatigue tests, both in-phase and out-of-phase, a fixed ratio between axial and shear strain range have been adopted, $\Delta\gamma=2\Delta\varepsilon$. The magnitude of strain range have been chosen so that the range of fatigue lives between about $2\cdot10^3$ and $2\cdot10^5$ cycles could be "explored". This is the range of fatigue life cycles which is likely to replicate the typical life of engine components for which the gas turbine industries already own fatigue experimental data.

2.4. Experimental results

High temperature multiaxial fatigue test results are shown in Fig. 5 in terms of the number of cycles to failure as a function of (normalised) applied strain range. Fatigue tests results are presented for each of the type of the performed test: pure axial, pure shear, axial/torsional in-phase and out-of-phase. Totally, a number of 48 valid fatigue test results are reported herein. However, due to confidentiality issues, applied strain range has been normalised, for each test condition, to the maximum applied strain range. The number of cycles to failure has been determined, when applicable, by 25% load (or torque) drop. Experimental fatigue test results show that, for a given applied strain range and test condition, scatter of results is limited, witnessing good quality replication and accuracy achieved during the setup phase.

By considering pure axial fatigue tests, experimental results reveal, as expected, a marked effect of positive mean stress (strain) state: at a given applied strain range, by increasing the mean stress (strain) by applying positive loading ratio, a decrease of fatigue life may be observed. However, it can be noted that fatigue life decrease seems relatively independent of applied mean strain. In fact, the biggest differences in fatigue lives are observed by comparing fatigue test results obtained under pure reversed loading (R_ε=-1) with those with a positive loading ratio (R_ε=0.5). On the contrary, comparing zero-to-tension (R_ε=0) and tension-tension (R_ε=0.5) fatigue test results, a marked difference cannot be observed. A likely explanation of this behaviour is that, at a given applied strain range, in the case of tension-tension (R_ε=0.5) fatigue tests, the maximum strain achieved during the test is greater than that observed during the zero-to-tension tests. Thus, due to higher plastic strains, a partial relaxation of mean stresses is observed and consequently a comparatively weaker effect of mean stress. From the torsion shear strain controlled

test results, it may be observed that the effect of applied mean shear strain is more evident in the lower cycle fatigue life regime, for which yield in shear occurs. Therefore, this observation does not seem to be in disagreement with commonly accepted experimental proof of the independence of torsional fatigue limit upon a mean shear stress [8]. Finally, multiaxial axial/torsional fatigue test results require a more in-depth and comprehensive discussion and a simple interpretation is not fit here. Even if the effect of applied mean stress (strain) is less pronounced, further information may be obtained by analysing the fatigue test results by applying suitable multiaxial fatigue life prediction criteria and methods [4], [5].

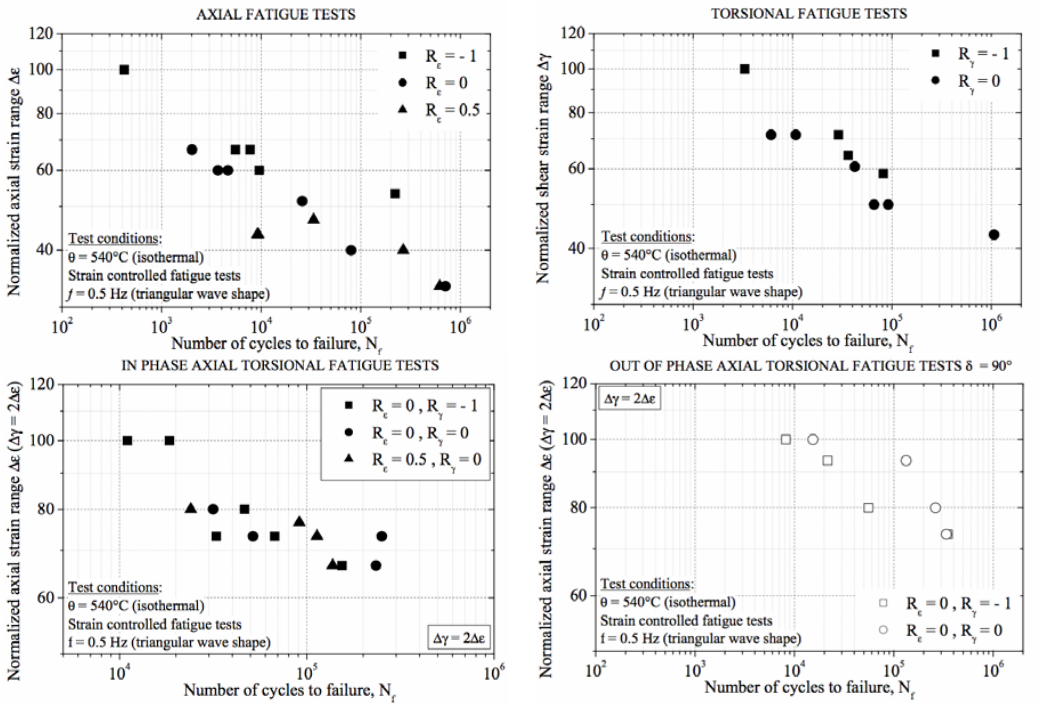

Fig. 5. (a) Axial, (b) torsional, axial/torsional in-phase (c) and out-of-phase (d) high temperature strain-controlled multiaxial fatigue test results.

3. Life prediction methodologies

In the literature, many methods have been proposed to reduce the complex multiaxial stress/strain state to an equivalent uniaxial condition, namely empirical formulas, equivalent stress or strain models, critical plane approaches and strain energy models. Most of these criteria can successfully be used for a simple stress state, i.e. uniaxial or in-phase loading, but their extension to a complex multiaxial state is often difficult. The experimental results reported in this study allow to check the predictive capabilities of different multiaxial fatigue criteria in the presence of a complex multiaxial stress and stain state, including non-proportional loading and multidimensional mean stress.

Historically, the first multiaxial cycle fatigue criteria have been based on the extension of (static) yield criteria, such as the von Mises criterion, in which the cyclic multiaxial stress or strain components are reduced to an uniaxial equivalent cyclic stress or strain. The main disadvantages of these criteria are: (i) the definition of a mean stress is vague in a multiaxial stress state and (ii) their application is limited to the case of fixed principal stress or strain directions during the loading cycle. However, because these models are well known, frequently used and not computationally intensive, a equivalent stress model, the modified Manson-McKnight model (MM), was evaluated

in this study. This model was selected due to its current application in life prediction and durability assessment of aircraft engine components [12] and because it has demonstrated good correlation with multiaxial test results [4].

In the so–called critical plane approaches, quantities related to the mechanism of formation of fatigue cracks under multiaxial loading are inserted explicitly in the formulation of the criteria: a combination of normal and shear stresses or strains acting on particularly oriented planes, on which fatigue cracks are likely to nucleate, is chosen as the critical parameter for assessing the fatigue life of components submitted to multiaxial cyclic loading. The critical plane approach is given a physical justification based on the observations of nucleation and early growth of fatigue cracks but, in most cases, its adoption is limited by the need of developing complex multiaxial material models and by the computational effort for large missions with multiaxial stresses that may be non proportional. Currently, the critical plane criteria appear to be receiving the most attention because of their good correlation with multiaxial stress data.

A number of critical plane models have been proposed in literature for crack nucleation life prediction. Two critical plane models was selected in this study: the Smith-Watson-Topper model (SWT) and the Fatemi-Socie model (FS). The SWT model is well-suited for tensile cracking, while the FS model is better suited for modelling shear cracking behaviour. These models have been selected for their widely accepted capability to correctly predict the fatigue life for different materials over a wide range of life for both uniaxial and multiaxial applied stress state. More detailed review of multiaxial fatigue criteria can be found in references [5], [9], [10] and [11].

3.1. Selected multiaxial fatigue criteria

Different multiaxial fatigue life prediction criteria have been applied in terms of pseudo-stresses; pseudo-stresses are obtained by imposing a linear elastic behaviour of the material, i.e. by calculating the stress components by multiplying the applied strains by the appropriate elastic moduli. This approach is consistent with the cyclic behaviour of the material, for which an elastic shakedown is observed even for the highest strain amplitudes applied during the strain-controlled fatigue tests, and with the peculiar behaviour of the Inconel 718 alloy, for which the number of cycles at transition between a predominantly elasto-plastic and a mainly elastic behaviour is less than $5\cdot10^2$ cycles. This behaviour can be observed not only at room temperature but also at the temperature employed in the tests presented in this paper. As a consequence, since the observed fatigue lives concentrate in the range between $2\cdot10^3$ and $2\cdot10^5$, in the tests conducted in this study, the use of damage parameters based on pseudo-stresses can be considered as consistent with the observed material behaviour.

3.1.1. Manson-Mcknight model

In the Manson-McKnight model, the Mises equivalent stress criterion is used to derive the alternating uniaxial equivalent stress:

$$\sigma_{\mathrm{ALT}} = \frac{1}{\sqrt{2}}\frac{1}{2}\sqrt{\left(\Delta\sigma_x - \Delta\sigma_y\right)^2 + \left(\Delta\sigma_y - \Delta\sigma_z\right)^2 + \left(\Delta\sigma_z - \Delta\sigma_x\right)^2 + 6\left(\Delta\tau_{xy}^2 + \Delta\tau_{yz}^2 + \Delta\tau_{zx}^2\right)} \qquad (1)$$

while the equivalent mean stress is given by:

$$\sigma_{\mathrm{MEAN}} = \frac{1}{\sqrt{2}}\frac{1}{2}\beta\sqrt{\left(\delta\sigma_x - \delta\sigma_y\right)^2 + \left(\delta\sigma_y - \delta\sigma_z\right)^2 + \left(\delta\sigma_z - \delta\sigma_x\right)^2 + 6\left(\delta\tau_{xy}^2 + \delta\tau_{yz}^2 + \delta\tau_{zx}^2\right)} \qquad (2)$$

The stress range and the mean stress for each component of the stress tensor is defined as:

$$\Delta\sigma_{ij} = \sigma_{ij,\max} - \sigma_{ij,\min}; \quad \delta\sigma_{ij} = \sigma_{ij,\max} + \sigma_{ij,\min}$$

The sign of the equivalent mean stress in the Manson-McKnight model is defined by the term β, depending on the maximum and minimum principal stresses:

$$\beta = \frac{\Sigma\sigma_I + \Sigma\sigma_{III}}{\Sigma\sigma_I - \Sigma\sigma_{III}} \qquad \text{where} \qquad \sigma_{III} < \sigma_{II} < \sigma_I$$

where $\Sigma\sigma_I$ and $\Sigma\sigma_{III}$ are the sum of the first and third principal stresses, respectively, at the maximum and minimum points in the cycle:

$$\Sigma\sigma_I = \sigma_{I,\max} + \sigma_{I,\min}; \quad \Sigma\sigma_{III} = \sigma_{III,\max} + \sigma_{III,\min}$$

In the Manson-McKnight model, the detrimental effect of increasing mean stress is introduced by employing the Walker model, where $R=\sigma_{MIN}/\sigma_{MAX}=(\sigma_{MEAN}-\sigma_{ALT})/(\sigma_{MEAN}+\sigma_{ALT})$:

$$\sigma_{W,MM} = \frac{\sigma_{\mathrm{ALT}}}{(1-R)^{1-m}} = f_{MM}\left(N_f\right) = A_{MM}\left(N_f\right)^{b_{MM}} + C_{MM}\left(N_f\right)^{d_{MM}} \tag{3}$$

where the material parameters of the Manson-McKnight model $A_{MM}, b_{MM}, C_{MM}, d_{MM}$ and the Walker exponent m are identified by the best fit with uniaxial fatigue test results.

3.1.2. Smith-Watson-Topper (SWT) model

The Smith-Watson-Topper method was selected as a model for the critical plane approach in the case that the failure cracking mode is predominantly tensile. In the case of the material studied in this work, it's well know that cracks nucleate in shear, but early life is controlled by cracks growth on plane perpendicular to the maximum principal stress and strain. Smith et al. (see reference in [5]) proposed a relationship that includes both the cyclic strain range and the maximum stress. By applying the SWT model in the case of pseudo-stress, an equivalent stress :

$$\sigma_{SWT} = \sqrt{\frac{E\Delta\varepsilon\left(\bar{\theta},\bar{\varphi}\right)}{2}\sigma_{\max}\left(\bar{\theta},\bar{\varphi}\right)} = \sqrt{\frac{\Delta\sigma\left(\bar{\theta},\bar{\varphi}\right)}{2}\sigma_{\max}\left(\bar{\theta},\bar{\varphi}\right)} = f_{SWT}\left(N_f\right) = A_{SWT}\left(N_f\right)^{b_{SWT}} + C_{SWT}\left(N_f\right)^{d_{SWT}} \tag{4}$$

is obtained, where the critical plane, identified by the angles $\bar{\theta}$ and $\bar{\varphi}$, is the plane of maximum normal stress range and σ_{max} is the maximum normal stress on the maximum principal stress range plane. The material parameters $A_{SWT}, b_{SWT}, C_{SWT}, d_{SWT}$ are identified by the best fit with uniaxial fatigue test results with R=-1.

The SWT model can be used in the analysis of proportionally and non-proportionally loaded components made of materials that primarily fail due to Mode I tensile cracking. The maximum normal stress term in Eq.(4) makes the model suitable for describing mean stress effect on fatigue life.

3.1.3. Fatemi-Socie model

The Fatemi-Socie model was selected as a model for the critical plane approach in the case that the failure cracking mode is predominantly governed by shear [13]. Based on experimental observation, Fatemi and Socie [5] suggested a damage model that includes the cyclic shear strain amplitude modified by the maximum normal stress on the critical plane. In the case of the application of this model in terms of pseudo-stresses, an equivalent shear stress:

$$\tau_{FS} = \tau_a\left(\bar{\theta},\bar{\varphi}\right)\left(1 + k\frac{\sigma_{\max}\left(\bar{\theta},\bar{\varphi}\right)}{\sigma_y}\right) = f_{FS}\left(N_f\right) = A_{FS}\left(N_f\right)^{b_{FS}} + C_{FS}\left(N_f\right)^{d_{FS}} \tag{5}$$

can be derived, where the critical plane, identified by the angles $\bar{\theta}$ and $\bar{\varphi}$, is chosen as that experiencing the maximum amplitude of shear stress. The equivalent shear stress is defined by a combination of maximum shear stress amplitude and maximum normal stress on the critical plane. The material parameters $A_{FS}, b_{FS}, C_{FS}, d_{FS}$, k are identified by the best fit with torsional and uniaxial fatigue test results with R=-1.

3.2. Application to experimental results

The fatigue life calculation models of Manson-McKnight, Smith-Watson-Topper and Fatemi-Socie have been applied to the experimental fatigue test results of the present study. Once the reference fatigue life parameters have been identified on a specific set of the uniaxial test results, for every single test in the present study dataset, the

fatigue life have been calculated and compared with the experimentally observed one, Fig. 6. In addition to, the histograms of the frequency count of the logarithmic relative error index:

$$E_{\log}\%^{(i)} = \frac{\log N_{f,\exp}^{(i)} - \log N_{f,\text{calc}}^{(i)}}{\log N_{f,\exp}^{(i)}} \cdot 100$$

between the calculated ($N_{f,\text{calc}}$) and experimentally observed fatigue life ($N_{f,\exp}$) are also shown, see Fig. 6. In this way the dispersion of the predictions of each model can be observed. In particular it's worth noting that the logarithmic error index permits to appreciate when conservative or un-conservative fatigue life predictions are obtained. In fact:

$$\text{where } E_{\log}\%^{(i)} = \begin{cases} \geq 0 & \text{if } N_c^{(i)} \leq N_f^{(i)} \quad \text{conservative} \\ < 0 & \text{if } N_c^{(i)} > N_f^{(i)} \quad \text{un-conservative} \end{cases}$$

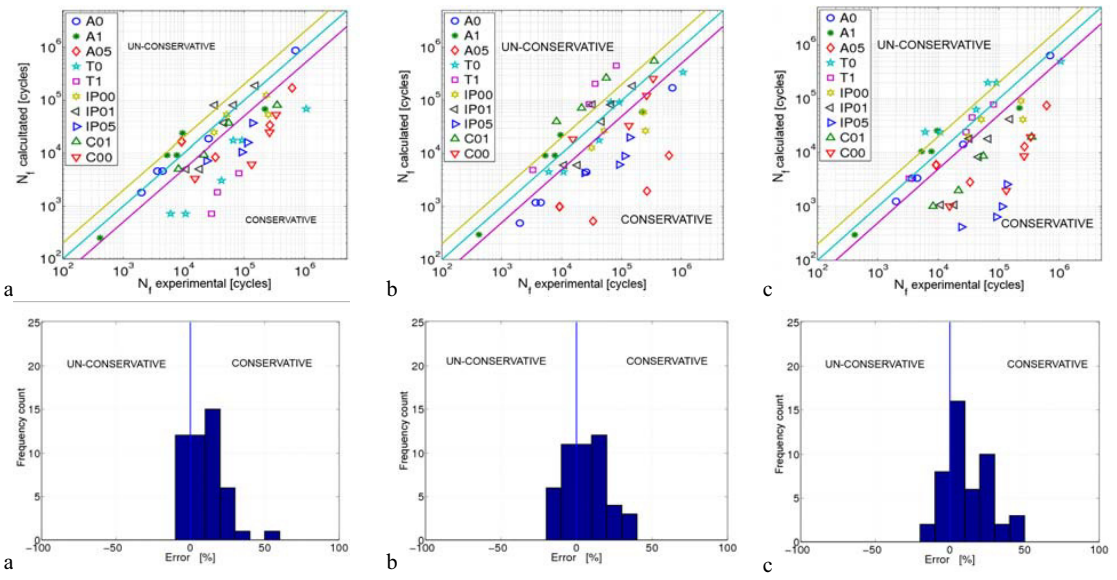

Fig. 6. Fatigue life calculations and corresponding distribution of logarithmic error index: (a) Manson-McKnight model; (b) SWT model; (c) Fatemi-Socie model.

4. Conclusions

In the present paper, test results of an extensive experimental high temperature multiaxial fatigue test campaign on a aerospace gas turbine engine alloy have been presented. Fatigue tests have been performed only after a carefully conducted setup phase, in order to ensure a reasonable replication of test results and to minimize, if possible, the scatter of fatigue test results that is typical of high performance nickel alloys. It needs to be underlined that the availability of a homogeneous and consistent set of multiaxial fatigue test results, with different combinations of axial and shear stresses and strains and loading ratios, is crucial for developing reliable fatigue life prediction criteria and methods. The presented experimental fatigue test results have given the possibility to carefully select and develop suitable fatigue life prediction methods that have been integrated in a specific fatigue

life calculation procedure which, after a phase of testing and benchmarking, could be employed as a fatigue design tool for aerospace gas turbine engines components.

References

[1] Harrison, G.F., Weaver, M.J., Life assessment of fracture critical aeroengine parts. In: Beynon, J.H. et al., editors. *Engineering Against Fatigue*. Balkema, Rotterdam, 1999, p. 713-720.

[2] Papadopoulos, I.V., Davoli, P., Gorla, C., Filippini, M., Bernasconi, A. A comparative study of multiaxial high-cycle fatigue criteria for metals. *Int. J. Fatigue*, 1997;**19**(3):219–235.

[3] Filippini, M., Foletti, S., Papadopoulos, I.V., Sonsino, C.M., A multiaxial fatigue life criterion for non–symmetrical and non–proportional elasto–plastic deformation. In: Carpinteri, A., de Freitas, M., Spagnoli, A., editors. *Biaxial/Multiaxial Fatigue & Fracture, ESIS Publication 31*. Elsevier, 2003, p. 383-400.

[4] Kallmeyer, A.R., Krgo, A., Kurath, P. Evaluation of multiaxial fatigue life prediction methodologies for Ti-6Al-4V. *J. Engng Mater. Tech., Trans. ASME*, 2002;**124**(2):229–237.

[5] Socie, D.F., Marquis, G.B., *Multiaxial Fatigue*. SAE International: Warrendale, PA; 2000.

[6] ASTM E 2207, Standard Practice for Strain-Controlled Axial-Torsional Fatigue Testing with Thin-Walled Tubular Specimens, ASTM International, West Conshohocken (PA), 2002.

[7] Thomas, G.B., Hales, R., Ramsdale, J., Suhr, R.W., Sumner, G. A Code of Practice for Constant Amplitude Low Cycle Fatigue Testing at Elevated Temperatures. *Fat. Fract. Engng. Mater. Struct.*, 1989;**12**(2):135-153.

[8] Davoli, P., Bernasconi, A., Filippini, M., Foletti, S., Papadopoulos, I.V., Independence of the torsional fatigue limit upon a mean shear stress. *Int. J. Fatigue*, 2003;**25**(6):471–480.

[9] Garud, Y.S. Multiaxial fatigue - A survey of the state of the art. *Journal of Testing and Evaluation*, *JTEVA*; 1981;**9**(3):165–178.

[10] McDowell, D.L. Multiaxial fatigue strength. In: *Fatigue and Fracture, ASM Handbook Vol. 19*, ASM Int., Materials Park, OH, 1996, p. 263–273.

[11] Ellyin, F. *Fatigue Damage, Crack Growth and Life Prediction*. Chapman & Hall: London; 1997.

[12] Gyekenyesi, J.Z., Murthy, P.L.N., Mital, S.K., NASALIFE—Component Fatigue and Creep Life Prediction Program. NASA/TM—2005-213886. National Aeronautics and Space Administration: Washington, DC; 2005.

[13] Socie, D.F., Critical Plane Approaches for Multiaxial Fatigue Damage Assessment. In: McDowell, D.L., Ellis, R., editors. *Advances in Multiaxial Fatigue, ASTM STP 1191*. ASTM, Philadelphia, 1993, p. 7–36.